Supplementing Experience-Based Platform System Robustness Requirements to Network Theory

E L Scheffers[a*], dr. P de Vos[a]

[a]Delft University of Technology, The Netherlands
*Corresponding author. Email: E.L.Scheffers@TUDelft.nl

Synopsis

Reduced crewing concepts require a higher level of control and integration of platform systems. A clear reliability assessment of these systems in early design stages reduces the need for alternations in later design stages but remains challenging to perform. This paper addresses the design of reliable and integrated onboard systems such as cooling water, power distribution, and control systems. Current approaches to making platform systems more reliable, such as redundancy, modularity (independent subsystems) and reconfigurability, are analysed from a network theory perspective. Current graph measures do not align with experience-based requirements for improving system robustness. Our method combines the principles of network theory and experience- and rule-based system requirements to provide a comprehensive framework for a reliability comparison of integrated multilayer platform systems (distributing more than one type of flow). The robustness requirements are translated into network metrics to facilitate a quantitative trade-off typical to the early stages of the design process. The case study offers a preliminary view of the system topology of a notional naval vessel, consisting of power distribution, cooling water distribution and control systems. The network metrics facilitate an assessment of the system's reliability compared to alternative system topologies with differentiating numbers of nodes, edges and density. This study finds varying dependencies of the robustness metrics on the network properties, shining new light on whether and how one should compare distribution system robustness.

Keywords: Onboard Distribution Networks; Design-Support Systems; Design Heuristics; Robustness

1 Introduction

Despite its critical role, the maritime industry operates largely in the shadows, only gaining fleeting visibility when incidents like the Baltimore Bridge collision capture headlines. These and other situations arise from a significant list of challenges facing the maritime industry, such as higher-risk shipping routes, operations in hostile environments, reduced crewing concepts and a need to mitigate local and global environmental impact. The first two challenges directly influence the lives of men and women onboard commercial and naval vessels. Therefore, it is essential to improve the survivability of these ships. Most naval vessels can be approached as complex systems of systems (Rigterink (2014)); enhancing the robustness of vital onboard distribution systems will likely lead to lower vulnerability and higher overall survivability (Habben Jansen (2020)).

This vulnerability has been a topic of study in various maritime applications, such as offshore and naval vessels. In previous work, Scheffers and de Vos (2024) used the difference between Dynamic Positioning (DP) class 2 and class 3 redundancy regulations (American Bureau of Shipping (2021)) to capture system robustness for ships equipped with DP systems. This robustness is defined by de Vos and Stapersma (2018) as "The ability of energy distribution systems on board of ships to withstand perturbations in system operation". The comparison was performed by modelling the DP systems as integrated networks. The systems were solely analysed from a logical architecture as defined by Brefort et al. (2018), focusing on the physical relations between components. Moreover, no differentiation between node and edge type has been taken into account. The robustness was measured using network metrics based on three reliability aspects: independent subsystems, component redundancy and distribution redundancy. The research used a single class 2 DP system and a single class 3 DP system as a case study to validate the assumptions from Clavijo et al. (2022). The study concluded that the network robustness metric "modularity" could be applied as a proxy for "independent subsystems" for this specific case study. However, no conclusion could be drawn regarding the other network robustness metrics nor regarding the applicability of these metrics on other onboard distribution system architectures.

Amongst the vital distribution systems, we consider electric energy distribution systems, cooling water distribution systems and sensor data distribution systems. One of the three main recommendations of this previous work was to broaden the general validity and applicability of the study. It was suggested to study networks of varying dimensions: what is the influence on robustness of adding additional components to the network?

Authors' Biographies

Evelien SCHEFFERS is a PhD candidate at the Department of Maritime & Transport Technology, Delft University of Technology. In her research, she focuses on the application of network metrics to robust on-board distribution system design

dr Peter DE VOS is assistant professor in marine engineering and director of studies of TU Delft's Maritime Technology MSc programme. In his research, he focuses on the design of robust on-board Power, Propulsion and Energy systems, including robust alternative fuel applications in marine Internal Combustion Engines.

 https://doi.org/10.24868/11147

Therefore, the goal of this paper is to verify whether a system becomes more robust if a component or connection is added to the network, i.e. increasing redundancy, and, if this is the case, which components have a pivotal position in this robustness enhancement. This current work studies the same five network robustness metrics as were used in the previous study since these metrics and the corresponding reliability aspects are directly based on DP regulations. The five metrics are 1) modularity, 2) effective graph resistance, 3) maximum flow, 4) clustering coefficient and 5) circuit rank and are further explained in Table 2. It is assumed that the network robustness metrics are also applicable in a broader sense to the vital distribution systems onboard naval vessels.

The verification is performed using the aforementioned network robustness metrics, which will be explained later in more detail. With this research aim in mind, the study consists of the generation of networks representing integrated onboard distribution systems (the logical architecture by Brefort et al. (2018)) and is based on an existing benchmark architecture (de Vos and Stapersma (2018)). The integrated systems consist of different system components and the number of these components is varied for the generated networks. Next, the effect of the number of components and connections with regard to the selected network robustness metrics is studied. The contribution of this work lies in studying the effect of the variation of network size on the robustness of onboard distribution systems.

2 Network Generation

Modelling the onboard distribution systems as networks is performed using the mathematical concept of graphs $G(V,E)$. These graphs are comprised of a set of nodes/vertices V (components) (Newman (2010)). The components relate to each other through a set of links/arcs/edges E (connections). In this work, the nodes represent system components such as pumps, engines, switchboards and computers. The edges represent tangible connections like cables, pipes and tubes. The physical architecture, as defined by Brefort et al. (2018), is not considered in this study, so physical properties like the cable length or capacity are not included in the scope. This is in line with studying system diagrams and facilitates analysis in very early-stage design before layouts or arrangements are known.

The benchmark system model of vital distribution systems onboard a notional frigate developed by de Vos (2018) serves as a foundation for examining the impact of component count on network robustness. This model identifies twelve distinct function types of system components, each categorised into a specific ”layer”. Roughly half of these layers comprise converter nodes, also known as ”converter layers,” which transform one flow, such as electricity, into another, such as cooling water. The remaining layers consist of hub nodes, or ”hub layers,” which facilitate flow distribution across the vessel without altering the flow itself. A cooling water pump exemplifies a converter node, whilst a switchboard is a hub node. Figure 1 shows the benchmark system model with its five distinct flows and twelve distinct node types. Converter nodes cannot directly connect to other converter nodes; instead, they must connect via one or more hub nodes to enable flow distribution. The second and final network constraint is that hub nodes can connect directly to each other and together form the distribution system for a given flow.

2.1 Erdös-Rényi random network generation

A number of possible topologies are generated to compare different system architectures. This generation starts with only the nodes from the benchmark system and an empty edge set: $G_0 = (V_{\text{benchmark}}, E = \emptyset)$. The physical boundaries, as introduced in the benchmark system, are translated to mathematical boundaries using the Erdös-Rényi (E-R) random graph model Newman (2010). For computational simplification purposes, it is assumed that a converter component is only connected to the hub layer “above” and “below” a given component and no other interrelations exist. Future research will include adding the additional interrelations as present in Figure 1, e.g. the sensor components requiring electric power, next to cooling. The edges are included with probability p, independently from every other edge. Since the physical networks onboard are assumed to be relatively sparse, the edge probability is set on a constant value of $p = 0.15$. This value reflects a sparse network whilst still facilitating sufficient edges to generate a connected network. Figure 2 shows a close-up of the upper three layers of the network to visually explain these boundary conditions in edge generation. Zooming in on the edge generation within the first three layers (diesel generator components DG, main switchboard components MSWB and transformer components (TF)), edges are generated within the following conditions. First, a subgraph S of graph G is defined as:

$$S(V_S, E_S) \subseteq G(V_{\text{benchmark}}, E = \emptyset) \tag{1}$$

with:

 https://doi.org/10.24868/11147

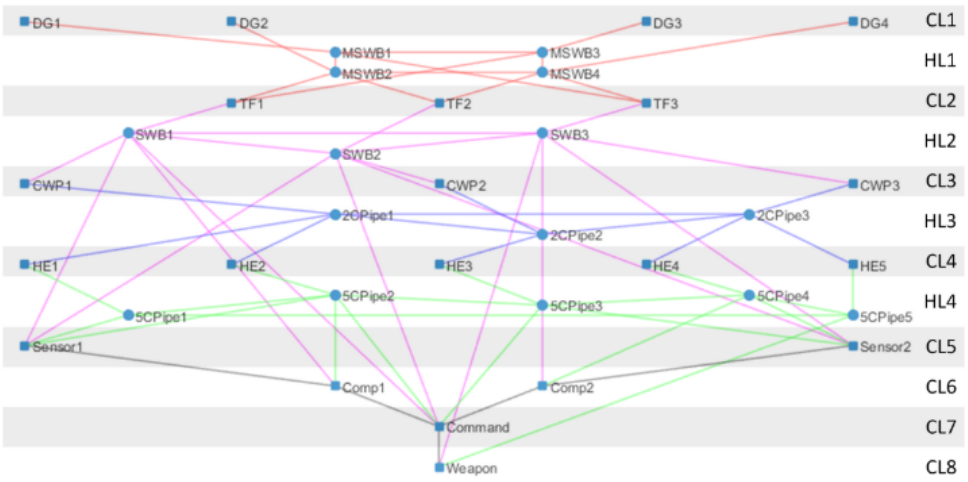

Figure 1: Benchmark energy and data distribution system model onboard a notional frigate (de Vos and Stapersma (2018)). The benchmark contains alternating converter layers (grey) and hub layers (white) and the five distribution flows 6600V AC (red), 400V AC (magenta), 2 °C cooling water (navy blue), 5 °C cooling water (green) and data (grey). The layers contain the following components: 1. diesel generator (DG), 2. main switchboard (MSWB), 3. transformer (TF), 4. switchboard (SWB), 5. cool water plant (CWP), 6. pipeline 2 °C (2Cpipe), 7. heat exchanger (HE), 8. pipeline 5 °C (5Cpipe), 9. Sensor, 10. Computer (Comp), 11. Command, 12. Weapon.

$$
\begin{aligned}
C_1 &= \{v \in V \mid \text{layer}(v) = \text{DG}\} \\
H_1 &= \{v \in V \mid \text{layer}(v) = \text{MSWB}\} \\
C_2 &= \{v \in V \mid \text{layer}(v) = \text{TF}\} \\
V_S &= C_1 \cup H_1 \cup C_2 \\
E_S &= \emptyset
\end{aligned}
\tag{2}
$$

where:

- C_i represents the node set of the i-th converter layer.
- H_i represents the node set of the i-th hub layer.

2.1.1 *Edge generation*

Now, edges are generated connecting the first (converter) layer to the first (hub) layer by means of an E-R random bipartite graph, i.e. no edges are generated within a layer, only between layers:

$$E_{C_1 \to H_1} = \{(c,h) \mid c \in C_1, h \in H_1, \text{ with } p = 0.15\} \tag{3}$$

To ensure that all converter components actively participate in the network, all converter nodes are ”required” to be connected to at least one hub node within this E-R bipartite graph:

$$\forall c \in C_1, \exists h \in H_1 \text{ such that } (c,h) \in E_{C_1 \to H_1} \tag{4}$$

Contrary to converter layers, the hub nodes are connected within the layer. These edges are generated using an E-R random graph:

$$E_{H_1} = \{(h_1,h_2) \mid h_1, h_2 \in H_1, \text{ with } p = 0.15\} \tag{5}$$

where the edges form a path between all hub nodes within the layer so that the hub layer is a connected graph. This requirement stems from the engineering practice of making distribution between hub nodes possible and often controllable via e.g. switches and valves. The connectivity is affirmed by:

$$\forall h_1, h_2 \in H_i, \exists \text{ a path from } h_1 \text{ to } h_2 \tag{6}$$

The last edge set within subgraph S is the E-R bipartite graph from the hub layer to the converter layer, repeating the concept of Equation 3 and 4.

 https://doi.org/10.24868/11147

$$E_{H_1 \to C_2} = \{(h,c) \mid h \in H_1, c \in C_2, \text{ with } p = 0.15\} \tag{7}$$

$$\forall c \in C_2, \exists h \in H_1 \text{ such that } (c,h) \in E_{C_2 \to H_1} \tag{8}$$

The combined edge set E_S of the graph $S(V_S, E_S$ is:

$$E_S = E_{C_1 \to H_1} \cup E_{H_1} \cup E_{H_1 \to C_2} \tag{9}$$

One should note that edges within this network have no flow type, direction or other physical properties (despite the obvious practical relevance and application of the connections); they simply represent an existing connection between two components. Physical properties make the network more realistic, however, unexpected and useful mathematical patterns might not be found.

2.1.2 Node addition

This study includes the influence of the number of components on robustness. Therefore, this network attribute should change for different generated graphs. To facilitate this, a random number $k \in 0, 1, 2$ nodes are added to each layer. This allows for a theoretical maximum of $n_{layers} \cdot k_{max} = 11 \cdot 2 = 22$ additional nodes in the graph. Since k is randomly determined for all graphs and layers, the likelihood of a generated network with $36 + 22$ nodes is slim. Figure 3 shows the upper three layers with the maximum number of nodes added to each layer ($k_1 = k_2 = k_3 = 2$). Visually, the added nodes are positioned in line with the existing nodes. Since the node addition is part of the input node-set V, the edge generation automatically includes the added nodes.

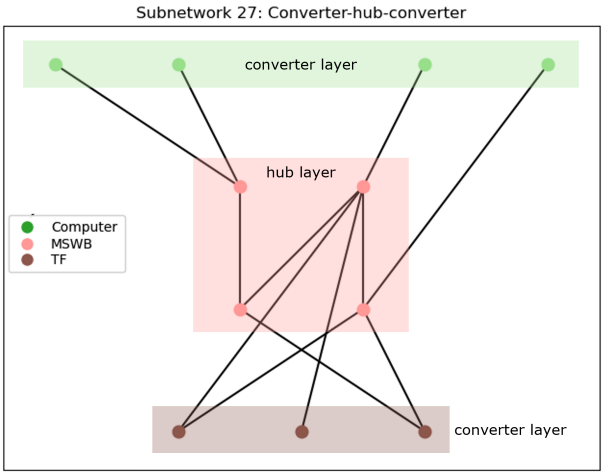

Figure 2: Upper three layers of the integrated system with the original number of nodes. The converter layers (green and brown) are both connected to the hub layer with an E-R random bipartite graph, connecting all converter nodes to at least one hub node. Within the hub layer (pink), an E-R connected graph is generated, which in its place connects the entire graph.

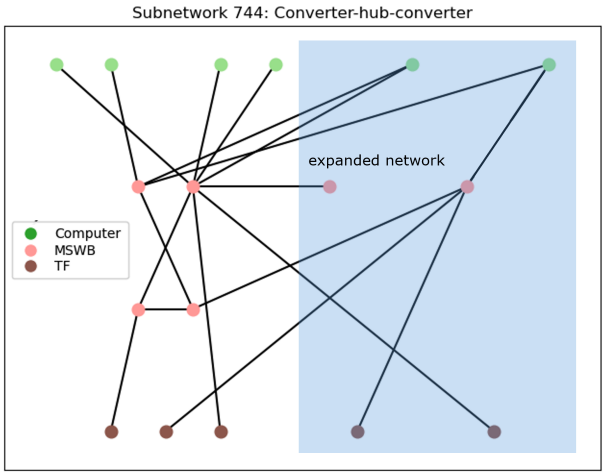

Figure 3: Upper three layers of the integrated system, each (randomly) expanded with two additional nodes highlighted with the blue box. For this generated network, all three layers have two additional nodes so $k_1 = k_2 = k_3 = 2$.

2.2 Generated network overview

Using the E-R random graph model, 2500 networks of the full 12 layers have been generated. The density (Equation 10) indicates the relation between the existing edges $|E|$ and the possible maximum number of edges. However, this does not take into account the limitations imposed by the network generation algorithm regarding the possible connections between nodes.

$$d(G(V,E)) = \frac{2|E|}{|V|(|V|-1)} \tag{10}$$

Table 1 shows the total number of nodes and edges, the network density of the undirected network, and the number of nodes per layer. The lower bound of the layer dimensions is equal to the network dimension of the

 https://doi.org/10.24868/11147

Table 1: Minimum and maximum number of nodes, edges, and network density with layer types. The network density is calculated as the ratio of existing edges divided to the total possible number of edges.

Name	Minimum [-]	Maximum [-]	Layer
Nodes	36	50	-
Edges	45	77	-
Density	0.055	0.094	-
Diesel Generator (DG)	4	6	Converter
Main Switchboard (MSWB)	4	6	Hub
Transformer (TF)	3	5	Converter
Switchboard (SWB)	3	5	Hub
Cool Water Pump (CWP)	3	5	Converter
2°*C* Pipe (2CPipe)	3	5	Hub
Heat Exchanger (HE)	5	7	Converter
5°*C* Pipe (5CPipe)	5	7	Hub
Sensor	2	4	Converter
Command	2	4	Hub
Computer	2	2	Data

original benchmark system de Vos and Stapersma (2018). The column "Layer" shows the alternating layer types. One should notice that the final layer, the data type computer layer, has a constant number of nodes ($|E|_{comp} = 2$). This is a simplified layer that includes both the command and weapon components from the original benchmark system in Figure 1. A constant number of nodes provides a consistent contribution to the network robustness, resulting in no changing influence on the robustness metrics. Figure 4 and Figure 5 display two extremes of generated networks; the minimum and the maximum number of nodes and edges, respectively. It is not a necessity that these generated networks contain both extremes in nodes and edges within one network.

2.3 Network Robustness Metrics

The applied network robustness metrics are a proxy for three reliability concepts: component redundancy, distribution redundancy and independent subsystems. First, the aspect independent subsystems refers to "two or more component groups, each of which is capable of individually and independently performing a specific function" (American Bureau of Shipping (2021)). The second reliability aspect, component redundancy, is achieved by the installation of multiple (functionally equal) components (American Bureau of Shipping (2021)). The last aspect, distribution redundancy, refers to the presence of "independent alternative paths between source and demand nodes which can be used to satisfy supply requirements during disruption or failure of the main paths" (Goulter (1987)). An overview of the applied network robustness metrics to estimate the system robustness of the generated networks is shown in Table 2.

3 Network database analysis

The generated network analysis is performed using the following steps. First, the relation between the metrics, number of nodes, edges and network density is visually inspected using a pairplot. This forms the initial step in understanding and getting familiar with the generated network database. Next, a Pearson correlation heatmap presents the linear relation between the metrics, network attributes and layer dimensions. This indicates the strength of positive and negative linear relations between the different studied network aspects. The third step is to study the influence of the number of nodes of each layer using a sensitivity analysis. Lastly, the use and applicability of the selected robustness metrics are evaluated using a second sensitivity analysis.

3.1 Pairplot and kernel density estimate

The pairplot in Figure 6 shows the five network robustness metrics, the number of edges, and the network density (Equation 10) on the x-axis and y-axis. What becomes clear from the colour gradient in the rows "Numedges" (number of edges) and "Density" is the direct relation between the edges and density, and the nodes: with an increase in nodes, the number of edges increases whilst the density decreases. Another apparent relation between the number of edges and the circuit rank in row "Numedges". Since both the number of nodes and the number of edges are directly and linearly present in the equation for circuit rank, this is a highly predictable relation.

 https://doi.org/10.24868/11147

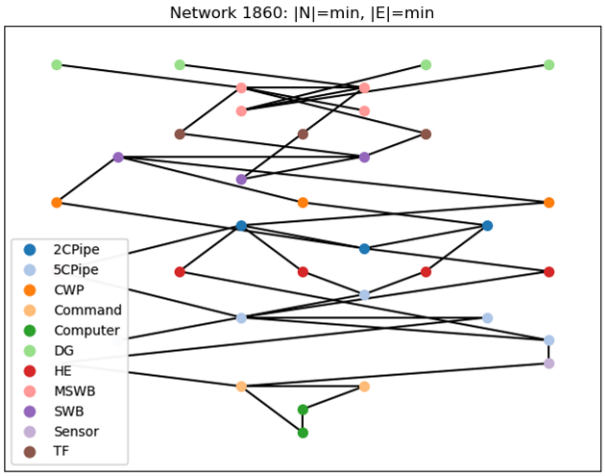

Figure 4: Generated network 1860 with the minimum number of nodes $|V|_{min} = 36$ and edges $|E|_{min} = 45$. The number of nodes corresponds to the number of nodes of the original benchmark system.

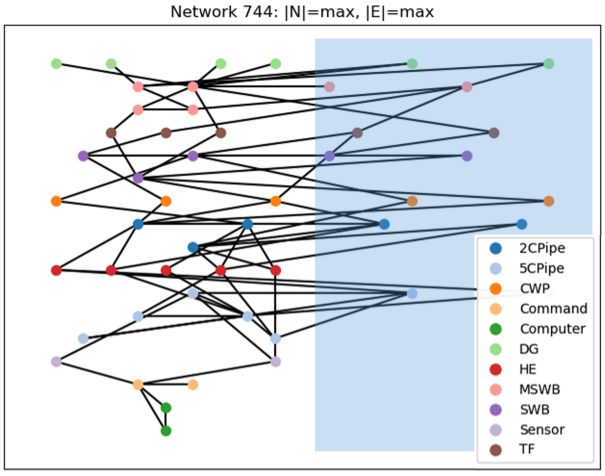

Figure 5: Generated network 744 (also shown in Figure 3) with the maximum number of nodes $|V|_{max} = 50$ and edges $|E|_{max} = 77$. With 14 additional nodes (highlighted in the blue box), the maximum of 20 additional nodes is not part of the generated network set.

Table 2: The calculation approach of the five selected network robustness metrics. The second column shows the three reliability aspects as defined based on the difference between the American Bureau of Shipping (2021) dynamic positioning class 1, 2 and 3 regulations.

Robustness metric	**Reliability aspect**	**Calculation**	**Method notes**
Modularity (Newman and Girvan (2004))	Independent subsystems	$Q_G = \frac{1}{2m}\sum_{ij}\left[A_{ij} - \frac{k_i k_j}{2m}\delta(c_i, c_j)\right]$	Partitioning using Leiden Algorithm (Traag et al. (2019))
Effective Graph Resistance (Ellens et al. (2011),Ellens and Kooij (2013))	Component redundancy	$R_G = \sum_{1\leq i\leq j\leq N} R_{ij} = N\sum_{i=2}^{N}\frac{1}{\lambda_i}$	λ_i is the i-th eigenvalue of the Laplacian matrix
Maximum Flow Newman (2010)	Component redundancy	Cut set algorithm: the removal of this number of nodes disconnects the source node from the sink node	A single artificial operational source and sink node are added, respectively connected to all source nodes (DG layer) and all sink nodes (Computer layer)
Clustering Coefficient Newman (2010)	Distribution redundancy	$c_G = \mathrm{Tr}(A^3)\left(\sum_{i=1}^{N} k_i(k_i-1)\right)^{-1}$	k_i is the number of direct neighbours of node i
Circuit Rank	Distribution redundancy	$r_G = \lvert E\rvert - \lvert V\rvert + \lvert C\rvert$	$\lvert C\rvert$ is the number of connected components, which is 1 for all networks since they are generated as connected networks

 https://doi.org/10.24868/11147

The plots showing the interrelations between the five network robustness metrics (the upper five rows and the leftmost five columns) are scattered; there seems to be no direct and strong relation based on this figure. This statement also seems to be valid for the relation between the number of nodes and the robustness metrics after studying the diagonal KDE plots of these metrics. The peaks of the different-coloured plots appear somewhat in the same location which shows that the value distribution of robustness metrics is comparable for networks with the different numbers of nodes. This suggests that the number of nodes does not play a key role in network robustness, indicating a preliminary answer to the main research goal. The remaining part of the network database analysis is likely to shine more light on this relation.

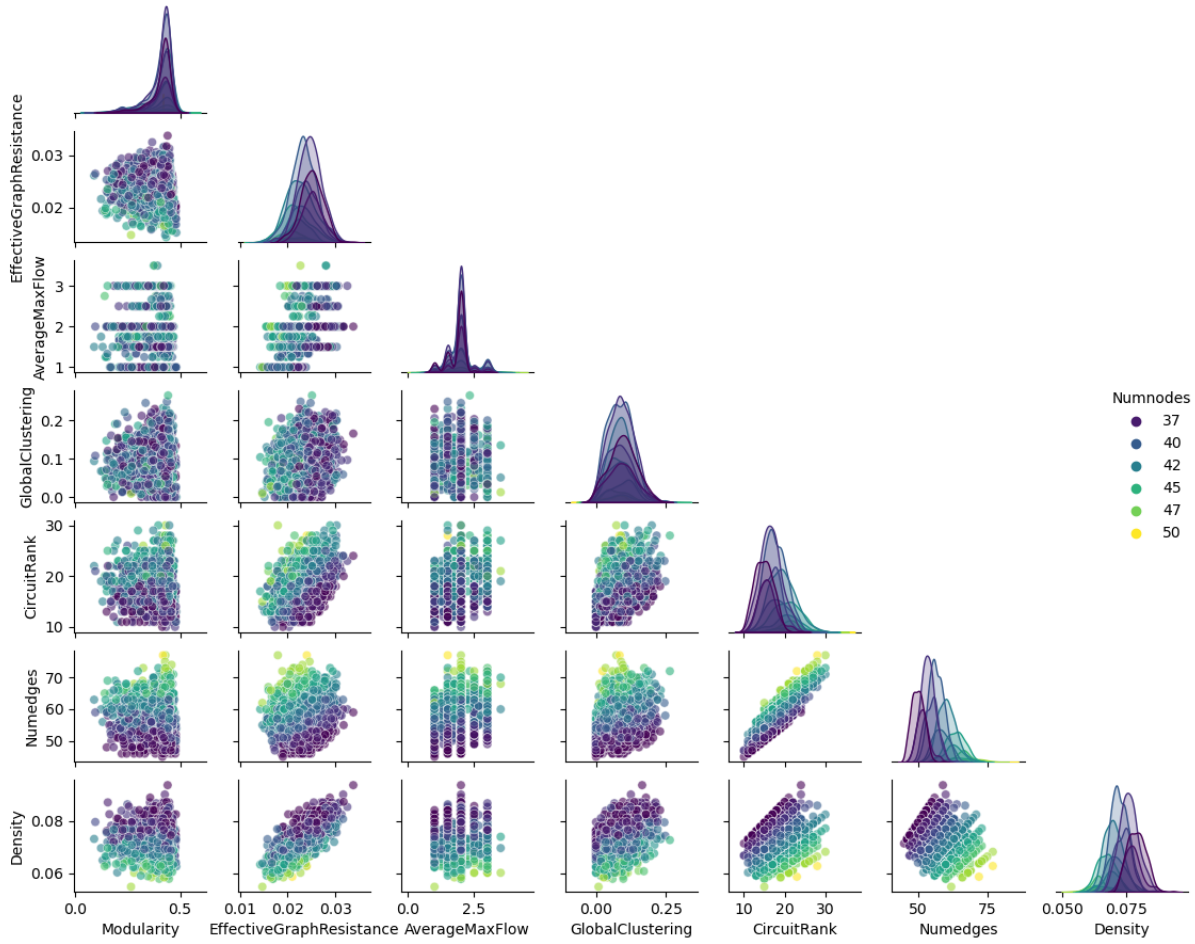

Figure 6: Pairplot showing the relation between robustness metrics and network dimensions. The diagonal plots show the kernel density estimate (KDE) of each metric. The colours represent the number of nodes (Numnodes) of each generated network, ranging from 36 (dark purple) to 50 (yellow).

3.2 Pearson correlation coefficient

The second analysis is a linear correlation analysis using the Pearson correlation coefficient $\rho_{X,Y}$. This coefficient indicates the strength of the linear positive or negative correlation between two variables and is calculated using

$$\rho_{X,Y} = \frac{\operatorname{cov}(X,Y)}{\sigma_X \sigma_Y} = \frac{\mathbb{E}\left[(X-\mu_X)(Y-\mu_Y)\right]}{\sigma_X \sigma_Y} \tag{11}$$

where:

$$\begin{aligned} &\operatorname{cov} \text{ is the covariance} \\ &\sigma_X \text{ is the standard deviation of } X \\ &\mu_X \text{ is the expected value (the mean) of } X \end{aligned} \tag{12}$$

Figure 7 shows a heatmap representation of the Pearson correlation coefficient. In line with Figure 6, the x-axis and y-axis show the network robustness metrics, the number of nodes, edges, and density. Moreover, the number

 https://doi.org/10.24868/11147

of nodes per layer is added to this heatmap. One should note that the positive scale does not surpass a coefficient value of $\rho_{max} \simeq 0.3$ where the strongest possible positive correlation is $\rho_{max,theory} = 1$. Therefore, even the darker red squares indicate, at best, a moderate positive relation strength. The strongest negative correlation value is $\rho_{min} \simeq -0.7$ with a theoretical minimum value of $\rho_{min,theory} = -1$. Again, this relation is not fully linear but can be considered as a strong correlation.

By studying the heatmap from left to right, two things stand out: first, the column "modularity" shows barely any significant correlation with any of the other studied network aspects. Second, modularity does show a somewhat stronger negative correlation with the number of cool water plant (CWP) components (row "Layer_CWP"), a converter layer with 3 to 5 nodes in the middle of the network. This correlation suggests that a lower number of CWP nodes leads to higher modularity, which is the desired effect for this metric. Understanding the ground for this relation will be studied in future research. An initial assumption is that this layer plays a critical role in determining the number of partitions formed in the modularity algorithm.

Effective graph resistance, the second column, must decrease to indicate an improvement in network robustness (Ellens et al. (2011)). Therefore, the number of nodes and particularly the number of nodes within hub layers (MSWB, SWB, 2CPipe, 5CPipe) have a positive influence on the effective graph resistance. Since the addition of a node will in itself increase the effective graph resistance if nothing else changes, this decreasing influence is surprising. If resistance were the only used metric, one might suggest that removing, for example, a heat exchanger to add additional pipes in the hub layers does improve the overall system robustness. The causal relation between these components is grounds for future research.

Some minor remarks remain, starting with the columns "average max flow" and "global clustering coefficient", which both seem mainly influenced by edge presence and, to a lesser extent, by the varying numbers of nodes. Since the circuit rank does have a positive relation with the number of nodes within layers, this could point to the fact that most triangles (three fully connected nodes) are formed between layers whilst more general cyclic structures are more often (also) found in hub layers. The remaining columns show less remarkable trends, with only the very strong negative correlation between density and number of nodes standing out. Since the number of nodes is present almost quadratic as the denominator in the density definition in Equation 10, this is completely expected.

3.3 Network dimension and layer sensitivity analysis

In this study, a Sobol′ (2001) sensitivity analysis is performed using a Saltelli sample space (Saltelli (2002), Saltelli et al. (2010)). The goal of this analysis is to evaluate the influence certain variables have on other variables. The sample space is determined by the number of input variables D and an input size indicator N, which is $N = 2^{15}$ for the three performed analyses.

3.3.1 Input: 13 network aspects (incl. layers), Output: 5 robustness metrics

Table 3 shows the results of the first sensitivity analysis, which contains thirteen input variables $D = 13$ and five output variables (the network robustness metrics) and has a sample size $N = 2^{15}$. The first conclusion drawn from this table, supported by Figure 8, is that effective graph resistance, global clustering and circuit rank are not or very limited influenced by the number of nodes. The network density and number of edges, two network aspects that are inherently closely related, are dominant factors in the expected values for these three network robustness metrics. Figure 6 and Figure 7 show results in line with this conclusion, which supports this analysis. However, this relation was not predominant in the previous parts of this research. Appendix A shows a figure for all five analysed metrics within this first sensitivity analysis.

A second finding is that in line with the first column of Figure 7, the number of CWP converter nodes has the strongest influence on the modularity metric. Some higher-order interaction is found between the number of edges, the density and the CWP layer. However, these effects are small compared to the first-order sensitivity relations. The sensitivity analysis of the maximum flow metric (Figure 13) is further studied as part of the second sensitivity analysis.

3.3.2 Input: 10 network aspects (only layers), Output: 5 robustness metrics

The second and third sensitivity analyses separate the input of the general network attributes, the number of nodes, edges and density, from the layer-based input. For the second performed sensitivity analysis, the density, total number of nodes and the total number of edges are disregarded as input variables. This facilitates a study into the influence of different layers, their character (converter nodes or hub nodes) and number of nodes on the network robustness metrics. The sample size is $N = 2^{15}$. Appendix B shows the five analysed metrics with the number of nodes per layer as sensitivity indices.

 https://doi.org/10.24868/11147

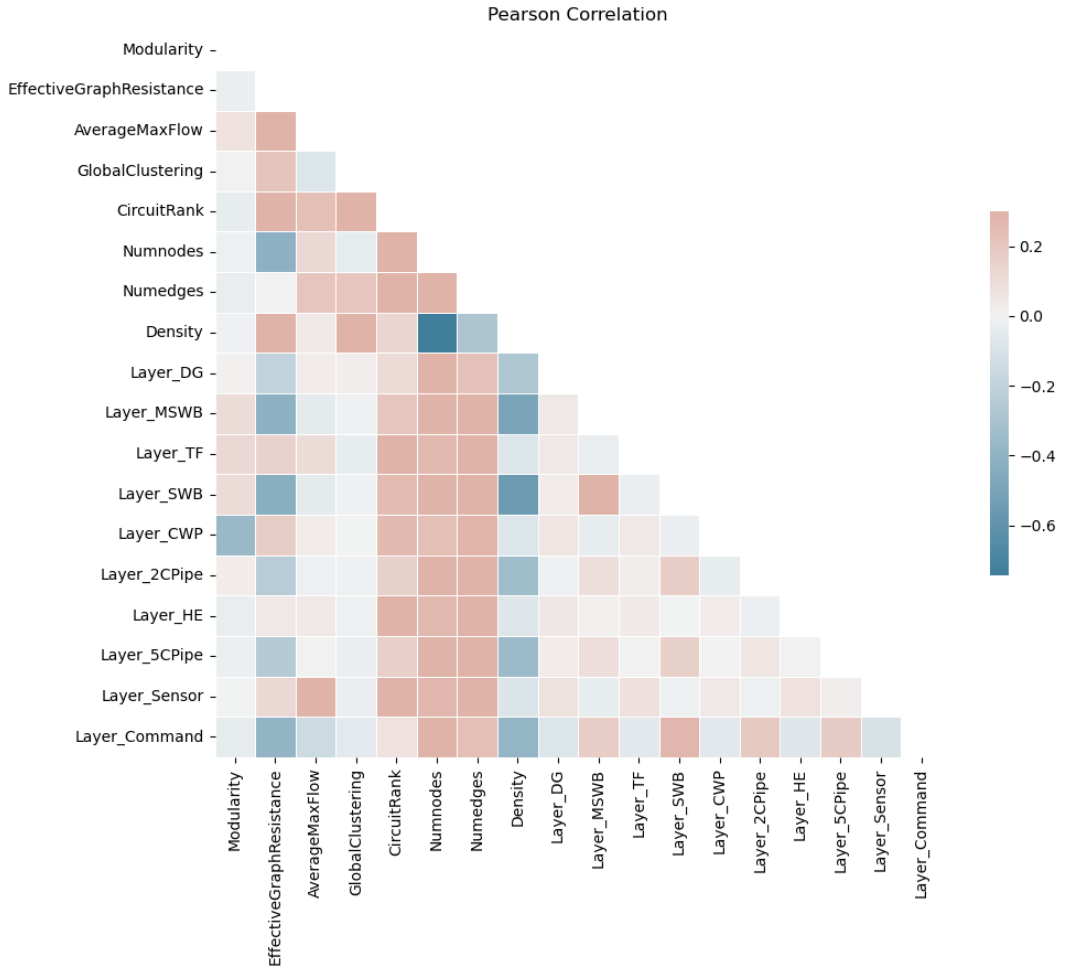

Figure 7: Pearson correlation heat map. The darker red squares indicate a positive linear relation, whereas the darker blue squares indicate a negative linear relation.

Maximum flow is almost fully determined by the sensor layer, which is in line with the first sensitivity analysis. The sensor layer is the smallest converter layer and is, therefore, a literal bottleneck in the flow from the operational source node (“above” the DG layer) to the operational sink node (”below” the Computer layer). Any additional component in the sensor layer facilitates a direct increase in flow through the system. Interestingly, the influence of the TF layer in the first sensitivity analysis (Figure 13) marginalises when the number of edges and density are not taken as input variables anymore. The plot “Second Order Sensitivity Indices for Average Max Flow” shows some weak second-order interaction between the TF layer and the density and sensor layer. However, the interaction seems to be predominantly part of the higher order.

Circuit rank is influenced by the number of nodes in all converter layers, whilst the number of nodes in hub layers plays a marginal role. This could be motivated by the boundary condition that all converter nodes must be connected to the previous and following hub layer. More nodes cause more edges, which is directly related to the number of circuits within the network.

3.3.3 Input: 5 network robustness metric, output: 5 network robustness metrics

The third sensitivity analysis focuses on the mutual influence of the network robustness metrics. For this analysis, the ”input variables” and ”output variables” change for each metric since the metric itself is considered input for the other metrics. Ideally, the five metrics have no influence on the other robustness metrics (Van Mieghem et al. (2010)). This orthogonality would indicate that the five metrics measure perfectly independent network properties and would, therefore, cover most of the character of the network when combined. However, the shared influence of density and number of edges on the metrics already suggests that the metrics are not fully independent. Appendix C contains five figures showing the first-order, second-order and total-order sensitivity analysis for each metric. As outlined earlier in 2, the five metrics correspond to three reliability aspects. For the sake of clarity and

 https://doi.org/10.24868/11147

Robustness metric	**Main input variable (secondary input variable)**	**Value (significant secondary value)**
Modularity	CWP Layer	$S_1 > 0.42$
Effective Graph Resistance	Density	$S_1 > 0.94$
Maximum Flow	Sensor Layer, (Transformer Layer)	$S_1 > 0.45$, ($S_1 > 0.14$)
Clustering Coefficient	Density, (Number of edges)	$S_1 > 0.72$, ($S_1 > 0.13$)
Circuit Rank	Number of edges, (Density)	$S_1 > 0.84$, ($S_1 > 0.14$)

Table 3: First order sensitivity analysis of network robustness metrics with 13 input variables. The second column shows the dominant variable and the second-most influencing variable with brackets; the corresponding values are given in the third column.

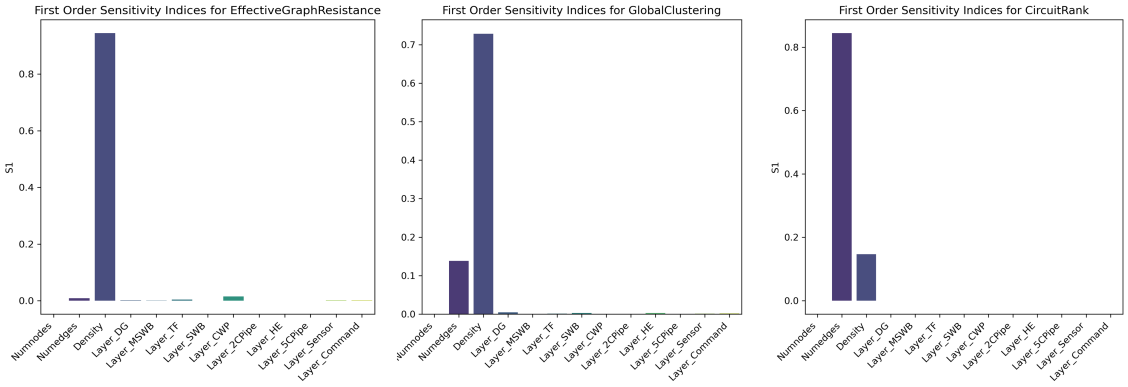

Figure 8: First order sensitivity analysis of the network robustness metrics Effective graph resistance, Global clustering and Circuit rank. The higher-order sensitivity analysis shows marginal values and is therefore not shown in this paper. The sample size of this analysis is set to $N = 2E15, D = 13$.

ease of reference, these aspects are reiterated here:

- **Independent subsystems** → Modularity
- **Component redundancy** → Effective graph resistance and Maximum flow
- **Distribution redundancy** → Clustering coefficient and circuit rank

It was initially expected that the number of nodes mainly influences the component redundancy and, to a lesser extent, the independent subsystems and distribution redundancy. However, Figure 12 shows limited influence of the number of nodes on the effective graph resistance. Therefore, this metric is possibly not the most suitable metric to measure component redundancy. The interesting part of the resistance metric is that it has the highest influence on modularity, maximum flow and circuit rank, respectively Figure 21, 23 and 25. The advantage of this metric is that it includes multiple aspects of other metrics, which is valuable if one metric is used as design or optimisation objective. However, a disadvantage is that the specific network properties that improve the value of the metric become less apparent. The global clustering coefficient and the circuit rank in Figure 24 and 25 are mutually influencing, which is in line with the expected behaviour as a proxy for distribution redundancy. The modularity sensitivity analysis in Figure 21 is in total order comparably equally influenced by the four other metrics. Together with the small influence of modularity on the other metrics, this is assumed to be an indication of the relative independence of this metric.

4 Conclusion and Discussion

The initial goal of this research was to determine the most robust integrated distribution system using network robustness metrics. The design space of these distribution systems showed variation in the number of nodes, edges, network density and network topology. In this research, 2500 connected networks have been generated using Erdös-Rényi random networks with boundary conditions mimicking common engineering practice. These networks are modelled based on the integrated distribution system on a notional frigate de Vos (2018). The physical boundary conditions have been translated to mathematical constraints, facilitating fast network generation and network analysis. The increase in case study size from two networks (Scheffers and de Vos (2024)) to 2500 has created a more thorough analysis and provided new insights with regard to what are ”good, safe and robust” distribution systems.

 https://doi.org/10.24868/11147

This analysis is performed using five metrics, each presenting certain robustness aspects based on dynamic positioning (redundancy) regulations. First, modularity is determined by two main characteristics. The first and main influence is the number of nodes in the cool-water plant (CWP) converter layer. The secondary relation is with the number of edges and the density. Modularity is, however, relatively independent of the other measured network aspects. This makes this metric interesting in its own right and not easily simplified by just using the network density. Future research should be directed at the partitioning algorithm and linking the mathematical modularity to operationally independent subsystems. The effective graph resistance is, to some extent, positively influenced by the number of hub nodes (more nodes lead to a lower resistance) but is mainly determined by the system density. This metric includes a variety of network properties and even when different-sized systems are compared, a lower resistance network with equal or more nodes indicates a higher robustness. Despite its relation to the number of nodes in the hub layers, resistance might not be the perfect proxy for component redundancy due to its tight relation with network density. The maximum flow between the operational source and sink node is determined by the system's "bottleneck layer", which is the sensor layer in the used case study. In terms of robustness, including this metric is valuable to identify this layer. However, it does not indicate the robustness of the complete system. The global clustering coefficient mainly identifies triangles between layers and has a significant overlap with the circuit rank. The triangles between layers could prove interesting when certain nodes require additional components. Future research into the application of the local clustering coefficient is therefore recommended. The last metric, circuit rank, indicates that the number of nodes in the converter layers has more influence on the distribution redundancy than the hub layers. However, the number of edges is the main input variable to this metric since this number is also directly related to the number of nodes. Therefore, this metric should be disregarded as a valuable robustness metric.

The overall goal of this research was to study the influence of adding nodes to the network on robustness. Based on the three performed analyses, all five metrics show, at best, a weak relation with the total number of nodes. Therefore, the conclusion is that simply adding a component will not inherently make the network more robust. To conclude, one should be very critical of the specific network property a metric is indicative of. Figure 9 and Figure 10 show the most robust networks based on the effective graph resistance and modularity, respectively. With proper awareness of their limitations, the network robustness metrics can provide valuable support in the design process of onboard distribution systems, contributing to reduced system vulnerability and, ultimately, improved overall ship survivability.

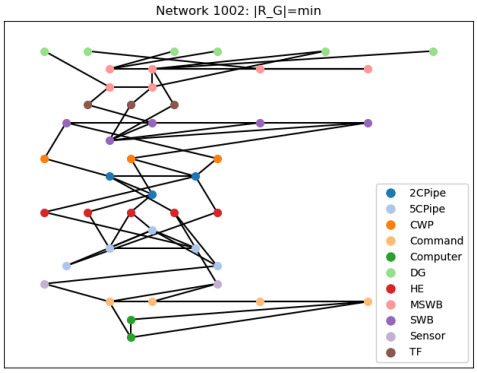

Figure 9: Generated network 1002 with minimum effective graph resistance, $R_G = 0.0143, Q = 0.433$.

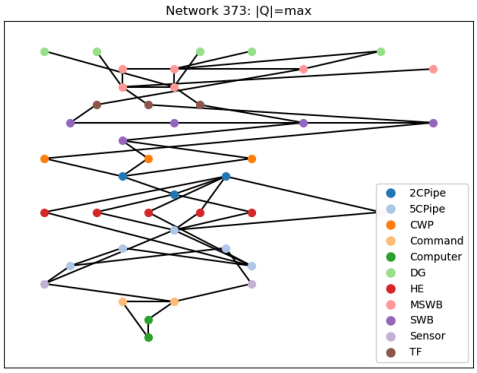

Figure 10: Generated network 373 with maximum modularity, $R_G = 0.0152, Q = 0.481$.

 https://doi.org/10.24868/11147

A Appendix: sensitivity analysis 1

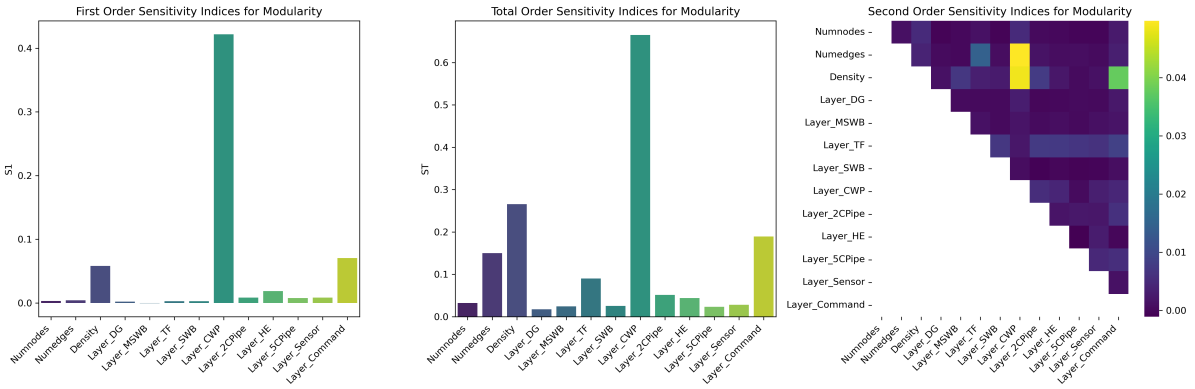

Figure 11: Modularity network robustness metric - sensitivity analysis: full sample space $N = 2E15, D = 13$.

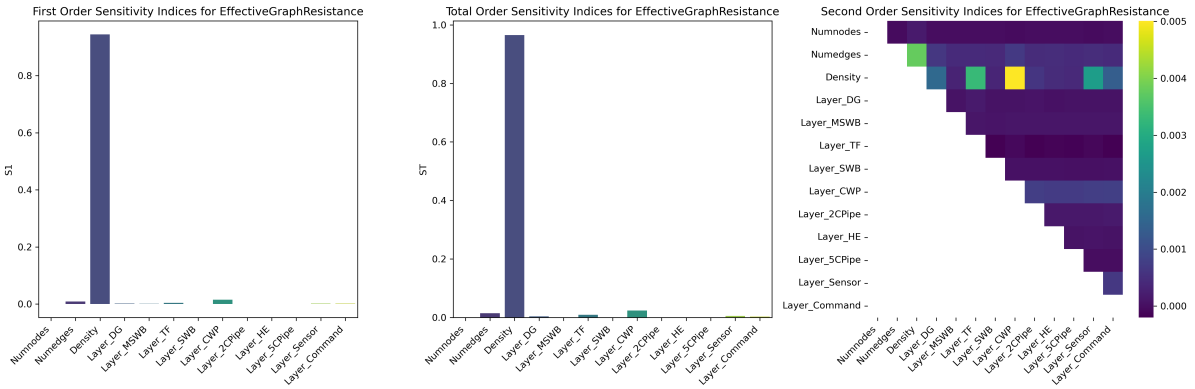

Figure 12: Resistance network robustness metric - sensitivity analysis: full sample space $N = 2E15, D = 13$.

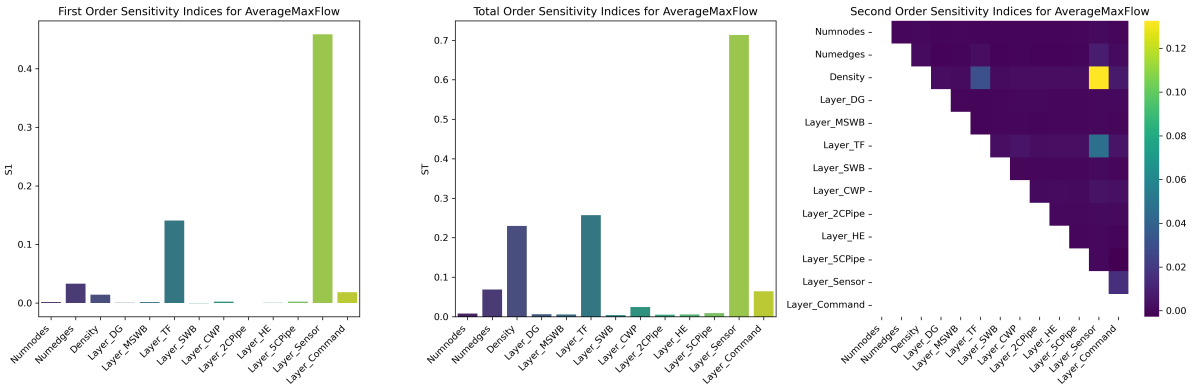

Figure 13: Max Flow network robustness metric - sensitivity analysis: full sample space $N = 2E15, D = 13$.

 https://doi.org/10.24868/11147

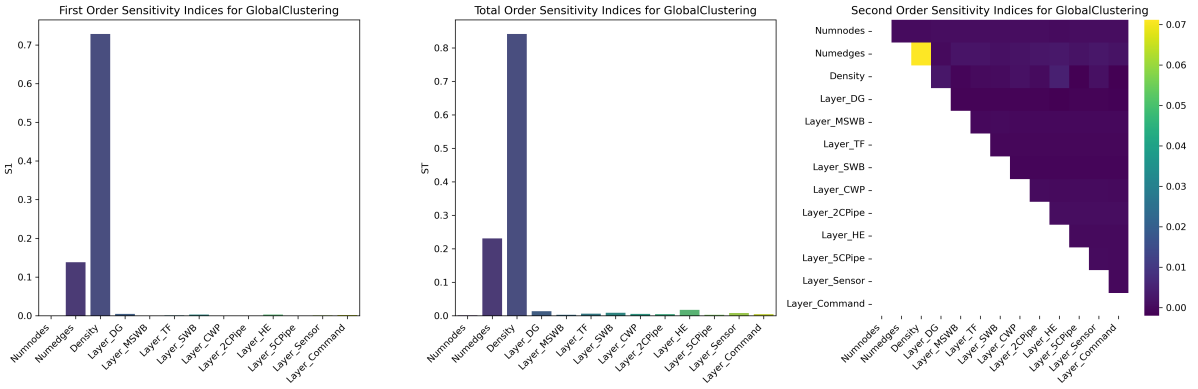

Figure 14: Clustering network robustness metric - sensitivity analysis: full sample space $N = 2E15, D = 13$.

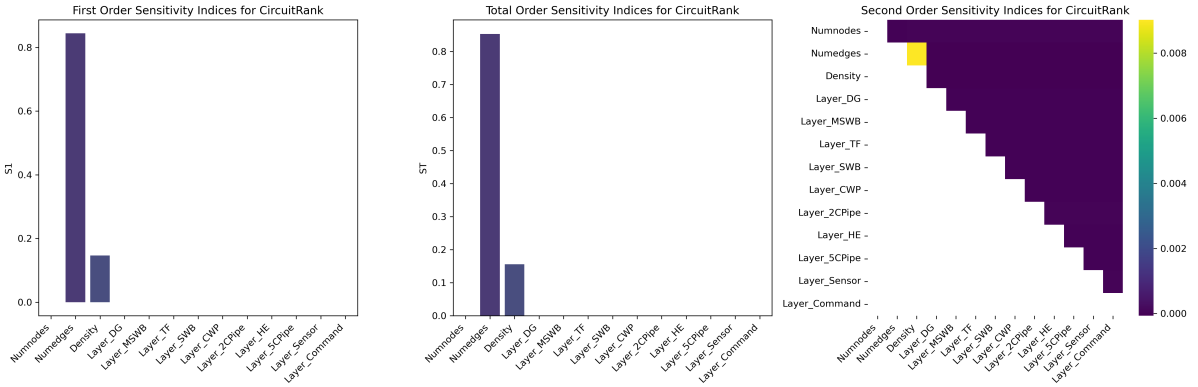

Figure 15: Circuit Rank network robustness metric - sensitivity analysis: full sample space $N = 2E15, D = 13$.

B Appendix: sensitivity analysis 2

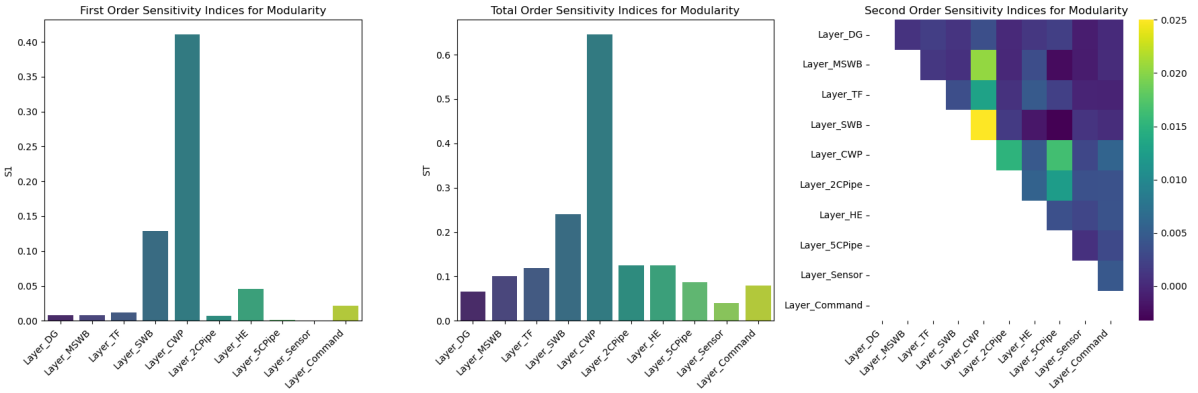

Figure 16: Modularity network robustness metric - layer sensitivity analysis: sample space $N = 2E15, D = 10$.

 https://doi.org/10.24868/11147

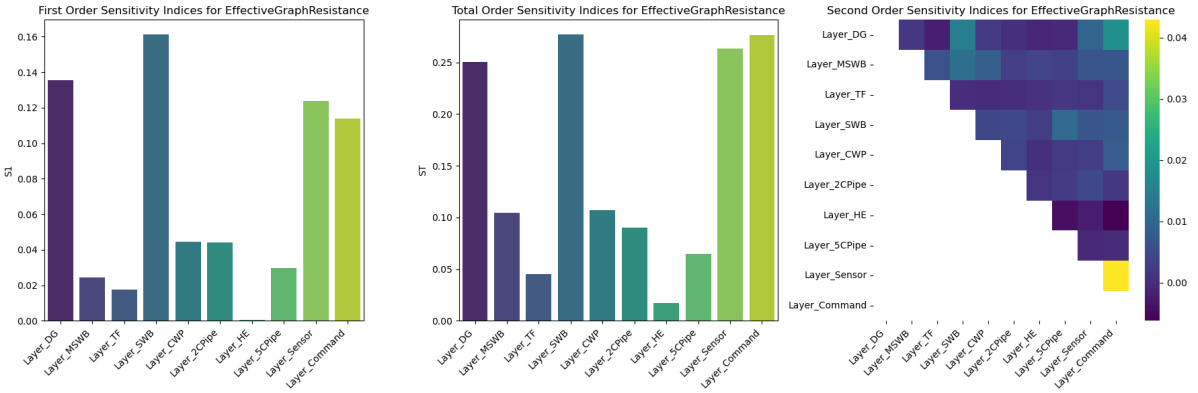

Figure 17: Resistance network robustness metric - layer sensitivity analysis: sample space $N = 2E15, D = 10$.

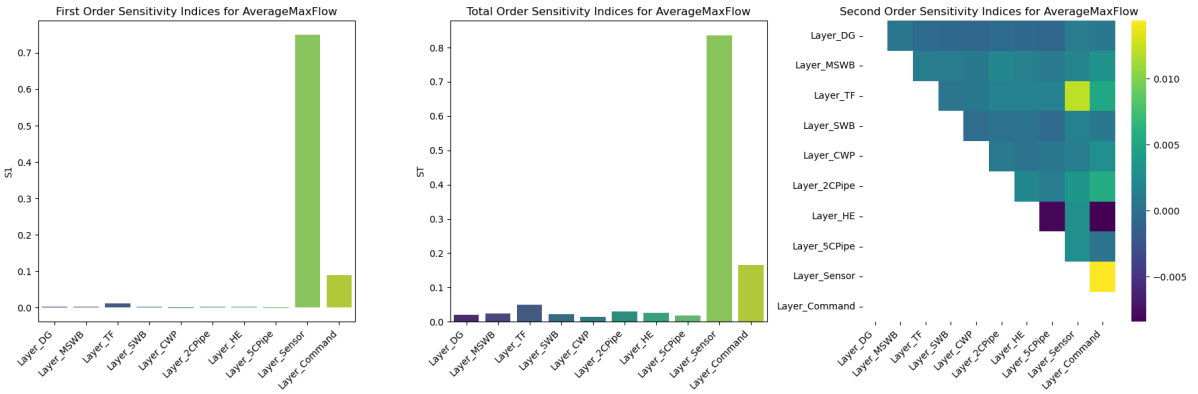

Figure 18: Max Flow network robustness metric - layer sensitivity analysis: sample space $N = 2E15, D = 10$.

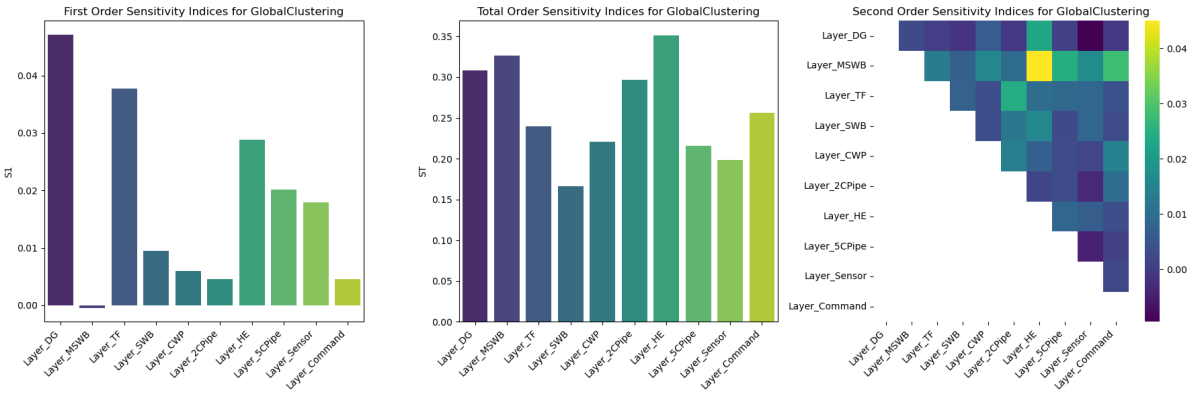

Figure 19: Clustering network robustness metric - layer sensitivity analysis: sample space $N = 2E15, D = 10$.

 https://doi.org/10.24868/11147

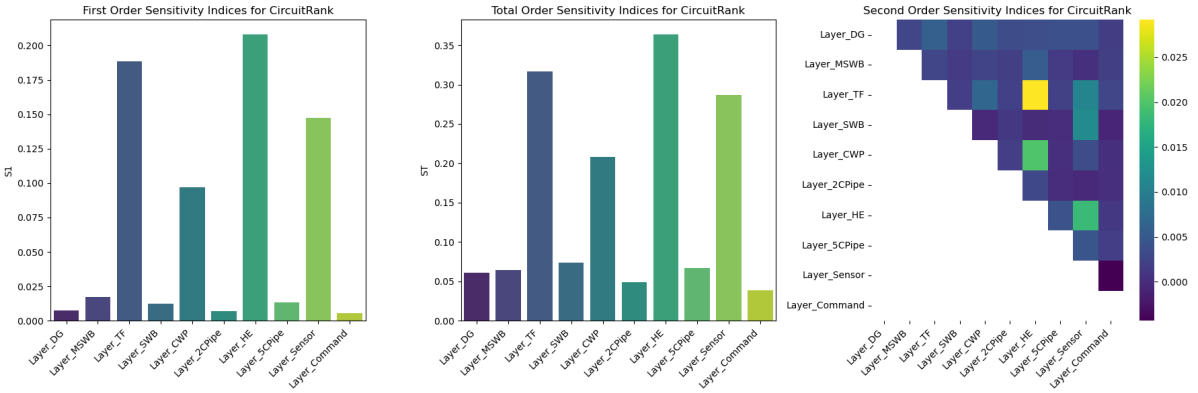

Figure 20: Circuit Rank network robustness metric - layer sensitivity analysis: sample space $N = 2E15, D = 10$.

C Appendix: sensitivity analysis 3

Figure 21: Modularity network robustness metric - mutual sensitivity analysis: sample space $N = 2E15, D = 4$.

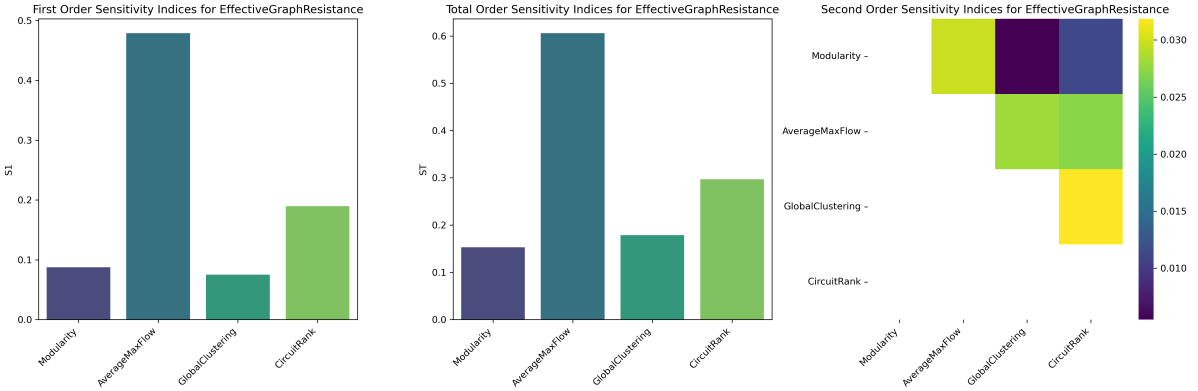

Figure 22: Resistance network robustness metric - mutual sensitivity analysis: sample space $N = 2E15, D = 4$.

 https://doi.org/10.24868/11147

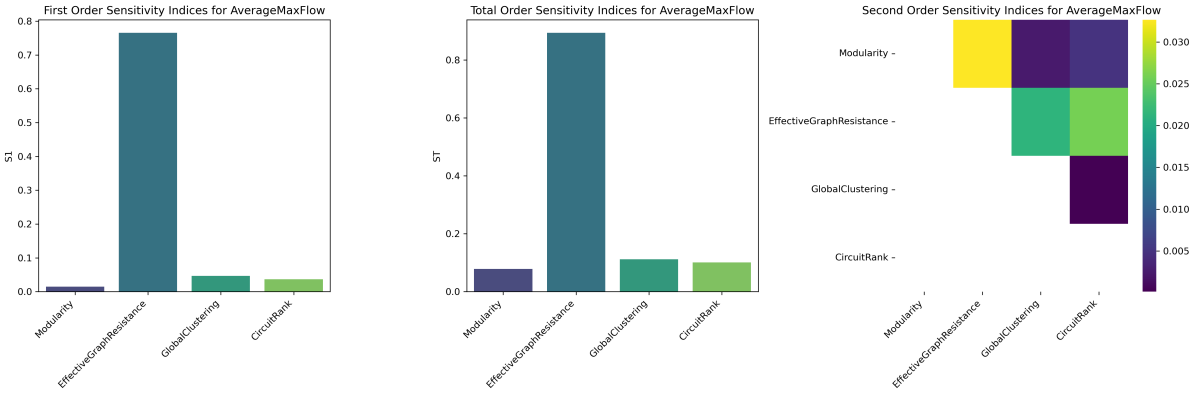

Figure 23: Max Flow network robustness metric - mutual sensitivity analysis: sample space $N = 2E15, D = 4$.

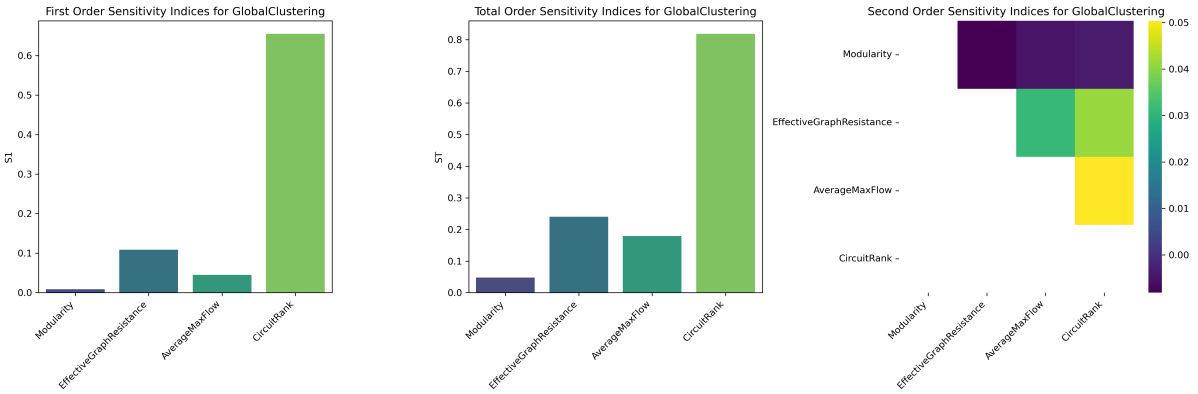

Figure 24: Clustering network robustness metric - mutual sensitivity analysis: sample space $N = 2E15, D = 4$.

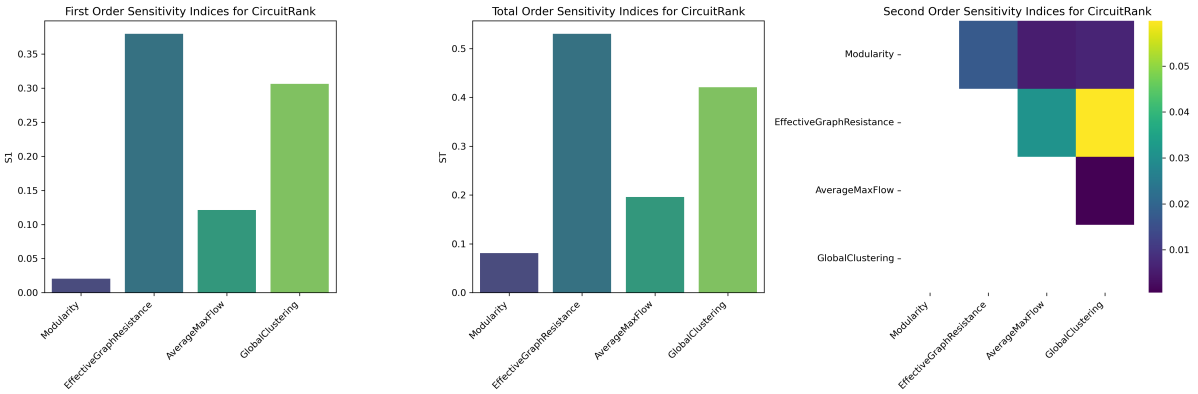

Figure 25: Circuit Rank network robustness metric - mutual sensitivity analysis: sample space $N = 2E15, D = 4$.

References

American Bureau of Shipping, 2021. Guide for Dynamic Positioning Systems 2021. Industry Guidelines. American Bureau of Shipping. Spring, USA.

Brefort, D., Shields, C., Habben Jansen, A., Duchateau, E., Pawling, R., Droste, K., Jasper, T., Sypniewski, M., Goodrum, C., Parsons, M.A., Kara, M.Y., Roth, M., Singer, D.J., Andrews, D., Hopman, H., Brown, A., Kana, A.A., 2018. An architectural framework for distributed naval ship systems. Ocean Engineering 147, 375–385. doi:10.1016/j.oceaneng.2017.10.028.

Clavijo, M.V., Schleder, A.M., Droguett, E.L., Martins, M.R., 2022. RAM analysis of dynamic positioning system: An approach taking into account uncertainties and criticality equipment ratings. Proceed-

ings of the Institution of Mechanical Engineers, Part O: Journal of Risk and Reliability 236, 1104–1134. doi:10.1177/1748006X211051805.

de Vos, P., 2018. On Early-Stage Design of Vital Distribution Systems on Board Ships. Ph.D. thesis. Delft University of technology. doi:10.4233/UUID:EB604971-30B7-4668-ACE0-4C4B60CD61BD.

de Vos, P., Stapersma, D., 2018. Automatic topology generation for early design of on-board energy distribution systems. Ocean Engineering 170, 55–73. doi:10.1016/j.oceaneng.2018.09.023.

Ellens, W., Kooij, R.E., 2013. Graph measures and network robustness. doi:10.48550/arXiv.1311.5064, arXiv:1311.5064.

Ellens, W., Spieksma, F., Van Mieghem, P., Jamakovic, A., Kooij, R., 2011. Effective graph resistance. Linear Algebra and its Applications 435, 2491–2506. doi:10.1016/j.laa.2011.02.024.

Goulter, I.C., 1987. Current and future use of systems analysis in water distribution network design. Civil Engineering Systems 4, 175–184. doi:10.1080/02630258708970484.

Habben Jansen, A., 2020. A Markov-based Vulnerability Assessment of Distributed Ship Systems in the Early Design Stage. Ph.D. thesis. Delft University of Technology. doi:10.4233/UUID:F636539F-64A5-4985-B77F-4A0B8C3990F4.

Newman, M.E.J., 2010. Networks: An Introduction. Oxford University Press, Oxford ; New York.

Newman, M.E.J., Girvan, M., 2004. Finding and evaluating community structure in networks. Physical Review E 69, 026113. doi:10.1103/PhysRevE.69.026113.

Rigterink, D.T., 2014. Methods for Analyzing Early Stage Naval Distributed Systems Designs, Employing Simplex, Multislice, and Multiplex Networks. Ph.D. thesis. University of Michigan. Michigan.

Saltelli, A., 2002. Making best use of model evaluations to compute sensitivity indices. Computer Physics Communications 145, 280–297. doi:10.1016/S0010-4655(02)00280-1.

Saltelli, A., Annoni, P., Azzini, I., Campolongo, F., Ratto, M., Tarantola, S., 2010. Variance based sensitivity analysis of model output. Design and estimator for the total sensitivity index. Computer Physics Communications 181, 259–270. doi:10.1016/j.cpc.2009.09.018.

Scheffers, E., de Vos, P., 2024. Supplementing Industry-Specific Dynamic Positioning Requirements to Network Theory. International Marine Design Conference doi:10.59490/imdc.2024.820.

Sobol′, I., 2001. Global sensitivity indices for nonlinear mathematical models and their Monte Carlo estimates. Mathematics and Computers in Simulation 55, 271–280. doi:10.1016/S0378-4754(00)00270-6.

Traag, V.A., Waltman, L., Van Eck, N.J., 2019. From Louvain to Leiden: Guaranteeing well-connected communities. Scientific Reports 9, 5233. doi:10.1038/s41598-019-41695-z.

Van Mieghem, P.V., Doerr, C., Wang, H., Hernandez, J.M., Hutchison, D., Karaliopoulos, M., Kooij, R.E., 2010. A Framework for Computing Topological Network Robustness .